

EXPERIMENTAL - THEORETICAL STUDY OF AXIALLY COMPRESSED COLD FORMED STEEL PROFILES

UDC 624.071.34=111

Miroslav Bešević* , Danijel Kukaras

Faculty of Civil Engineering Subotica, University of Novi Sad, Serbia
*miroslav.besevic@gmail.com

Abstract. *Analysis of axially compressed steel members made of cold formed profiles presented in this paper was conducted through both experimental and numerical methods. Numerical analysis was conducted by means of "PAK" finite element software designed for nonlinear static and dynamic analysis of structures. Results of numerical analysis included ultimate bearing capacity with corresponding middle section force-deflection graphs and buckling curves. Extensive experimental investigation were also concentrated on determination of bearing capacity and buckling curves. Experiments were conducted on five series with six specimens each for slenderness values of 50, 70, 90, 110 and 120. Compressed simply supported members were analyzed on Amsler Spherical pin support with unique electronical equipment and software. Besides determination of force-deflection curves, strains were measured in 18 or 12 cross sections along the height of the members. Analysis included comparisons with results obtained by different authors in this field recently published in international journals. Special attention was dedicated to experiments conducted on high strength and stainless steel members.*

Key words: *axially compressed members, experimental analysis, numerical analysis, finite element method, buckling curves, carbon steel, cold formed profiles, stainless steel, high-strength steel.*

1. INTRODUCTION

1.1. Analysis of the new results of high tensile and stainless steel

The use of cold-formed steel structures has increased rapidly in recent times due to significant improvements in production technology and the development of thin high-strength and stainless steel. The nominal yield limit of steel is in the range of 250 to 550 MPa, while the thickness of less than 1.00 mm is commonly used. Cold rolled steel sections have distinct structural stability problems, which are not observed in hot rolled sections. (Narayanan, Mahendran 2003) have presented detailed study of different cross-sectional thickness of $d=0.8-1.0\text{mm}$. Buckling and behavior of columns under full load is

numerically investigated with finite element and finite strip based software and the results are verified against experimental results and AS / NZS 4600 standard. (L. Gao, H. Sun, F. Jin, H. Fan). This research (B. Young, W. M. Lui, E. Ellobody, J. M. Goggins, B. M. Broderick, C. Muler and Y. Liu, B. Young) showed that columns made of cold formed profiles are very sensitive to the geometric imperfection, which implies a need to include it into design procedures. Investigation made by the author of this paper (Bešević, 2010) showed that similar conclusion can be made for carbon steel.

1.2. Analysis of the results of carbon steel

Axially compressed member is a member with compression force applied along its centroid axis. Geometrically perfect, straight axially compressed member does not exist. Such a member should not have any lateral deflection for loads less than critical. In reality lateral deflection occurs from the very beginning of the load application process, due to the bending caused by the initial curvature and eccentricity of the force. Due to the material imperfection and residual stresses as well as the variable yield point across the cross section, additional effects on lateral deflection for loads above the proportional limit emerge. The distribution of above mentioned stresses in comparison to the main section axes affects the distribution of yield zones. These effects, replaced by the equivalent geometric imperfection of the element can significantly reduce its load bearing limit. The main issue is to make sure that joints will not influence the stresses in the mid section of the member.

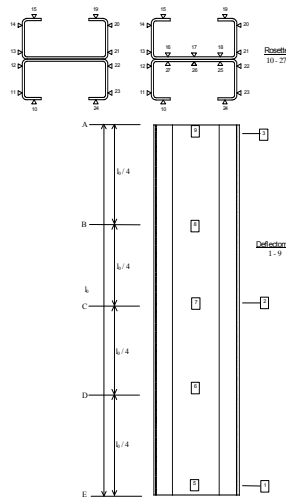


Fig. 1. Test layout



Fig. 2. Spherical bearing - Amsler type

The method used for testing of axially compressed built up members is the one defined by the European convention for obtaining the stress - strain curve with constant increase in force of 10 N/mm² per minute until the failure. The centroid of a cross section is the reference point for positioning of a specimen. Spherical bearing manufactured by Amsler was used for testing. It allows deflection in x and y direction. Fig. 2 represents the spherical bearing and fig. 1 testing layout of built up member formed by point welding of two cold formed lipped channels.

1.3. Pretesting

The EC-3 recommendations for experimental investigation give the following minimum of pretesting, measurements and testing equipment for testing of load and stability of axially compressed members:

1. Mechanical characteristics of the material obtained by tension tests and by stub column testing (completed for specimens U1 to U6, five series each).
2. Pretesting of specimens covered cross-section characteristics, dimensions of the web, flanges, width, diameter of corner curves, i.e exact features (area, momentum/radius of inertia/gyration). These measures were taken nine times in each of five sections along the specimen length.
3. Initial deflection i.e. straightness of the member for both axes in five sections along the specimen length.
4. Testing of residual stresses in a cross section of a member
5. Centric positioning of a specimen on the bearings
6. While testing axial compression capacity the following must also be tested:
 - limits,
 - diagram force-deflection for the midsection,
 - diagram force-dilatation for the midsection.

Testing of axial compression capacity was completed for five series of slenderness values equaling 50, 70, 90, 110 and 120. Lengths of built up members had the following values 122.11, 170.95, 219.79, 268.64 and 293.06 cm. Testing was completed in the laboratory of the Institute for Materials of Serbia on a 500 ton press. Electronic deflectometer Hottenger, type 50, connected to the UPM 60 device, was used to measure the application of force (fig. 3). For measurement of deflection along the x axis, as shown in the fig. 4, five deflectometers, placed along the length of samples, were used. For perpendicular direction three deflectometers were placed out of which two by the bearings and one in the midsection. Out of six specimens in the same series two were used to measure dilatations and the test force. Layout and number of the tapes was 12 or 18 tapes positioned in the midsection. The force application process and recording of the output results was the same for all series and all specimens, which is confirmed by the diagrams force-deflection and force-dilatation for series with constant values of slenderness. The results for cyclic loading, as well as maximum deflection values are shown on Fig. 4 the specimens U33.

2. INVESTIGATION PROCEDURE

Buckling tests for specimens with measurement tapes gave the date for diagrams critical test force - deflection and for other specimens the diagrams critical test force - maximum deflection. Centric positioning of the specimens was done with special attention and it required multiple observations and adjustments so



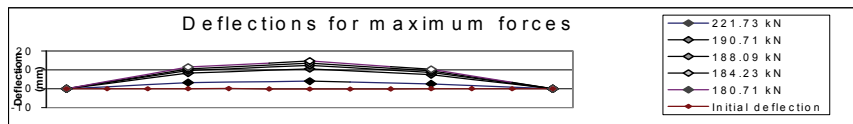
Fig. 3. Column samples during testing

that centroid of the end cross section and center of the bearing would match. Specimens were specially processed in order to have end cross sections perpendicular to their longitudinal axis. Their surfaces were processed by a face milling cutter. Centering has more influence with shorter specimens and lower values of slenderness. However, imperfections in centric positioning always influence the performance and to a certain extent load bearing capacity of a specimen. This is specially the case when taking into consideration the initial curvature of a specimen and low values of residual stresses where this influence can become dominant. From the very beginning of load application the member buckles, at first because of non-linear member geometry and later on because the material starts to behave in non-linear way. Data obtained by three types of experimental investigation gave the basis for calculations of the buckling curves - global failure limit, stub column test and elongation of the basic steel material.

Buckling test of 2C 90x45x20x2.5, built up member, formed by spot welding

Cyclic load (five cycles) for U33 specimen (series 3)

Force (kN)	Deflection (m m)												
221,726	0			3,28				3,99				2,56	0
190,714	0			8,27				10,60				7,42	0
188,090	0			9,61				12,32				8,62	0
184,229	0			10,51				13,48				9,44	0
180,715	0			11,45				14,67				10,27	0
Initial deflection	0	0,00	0,01	0,07	0,16	-0,05	-0,16	-0,16	-0,08	0,06	0,04	0,03	0



Relation force - deflection (reduced) for cyclic load

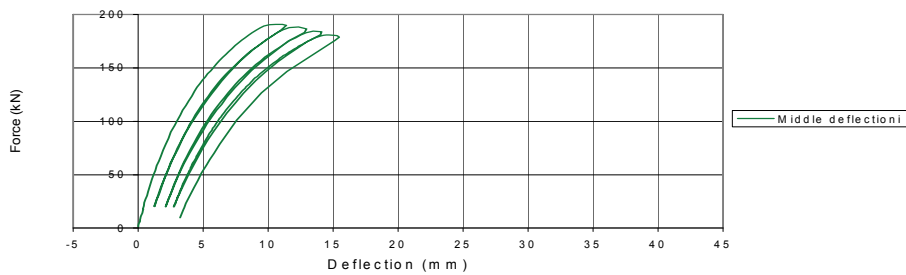


Fig. 4. Cyclic application of the load, diagrams and deflection table for the specimen U33

3. EXPERIMENTAL INVESTIGATION OF AXIALLY COMPRESSED MEMBERS FOR SLENDERNESS VALUES OF 50, 70, 90, 110 AND 120.

Obtained values for deflection were used to calculate the elasticity modulus. Measured values are similar on the same portions of the profile while at the opposite side they change orientation under the limit load. The force-deflection diagrams obtained like this show that strains on the compressed side of the section are magnified due to the residual stresses too, caused by manufacturing processes (cold rolling). Fig. 5 shows the diagram force-deflection for U56 specimens. (Besevic 1999).

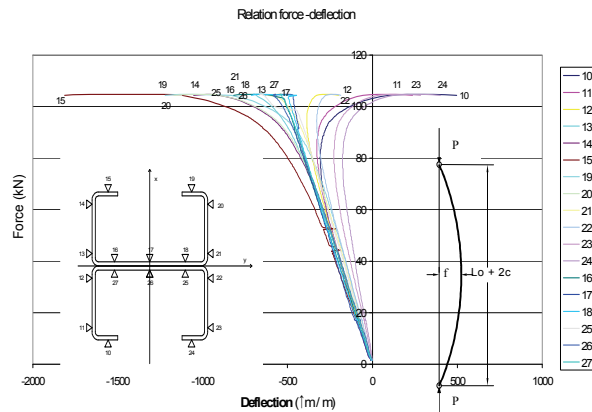


Fig. 5. Relation of force to deflection for U56 specimen

The results of experimental investigation of axial load bearing capacity of cold formed built up members 2C90.45.20.2,5 were compared to the European buckling curves. Obtained results are compared to the European buckling curves on the basis of stub column tests σ_t and elongation of the basic material Rel . The variations from the buckling curves A, B, C and D are marked specially with given percentages. The buckling line of axially compressed member relies to the initial imperfections, as proved by the buckling tests. Point welding was used to connect the two separate lipped channels, which remained non-deformed during the testing. The space between the spot connections was according to the Eurocode 3 recommendations.

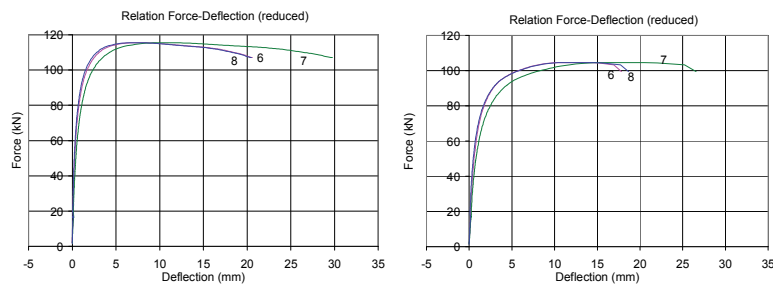


Fig. 6. Force/deflection ratio for test samples U56 and U61

Maximum limit of force deflection obtained in the test column and the corresponding shifts are given in table 1. Deflection test was continued with a reduction in the fall of the critical force and increase the deflection. For some samples of the pressure tests are performed to limit the separation of certain elements, and bringing connecting means (of point welded seams to break). This is to want to prove and establish the capacity coupling means without further detailed analysis. Links to some samples were left undisturbed and the maximum deflection of samples as you can see the pictures of samples.(Besevic 2010).

Table 1. Results of experimental investigation of axial load capacity of the complex stick 2C90.45.20.2, 5, and deviations from European deflection curves based on tests of short columns

Sample	σ_T (kN/cm ²)	A (mm ²)	I _y (mm ⁴)	λ_e	P ^F _{max} (kN)	σ_E (kN/cm ²)	σ_E / σ_T (kN/cm ²)	λ	Deviation from curve (%)				
									A	B	C	D	
U21	32.57	1021.622	570478.230	51.673	263.1818	25.76117	0.791	0.550	12.883	8.164	2.888	-6.272	-3.407
U22	32.57	1025.1	574815.611	51.695	254.9648	24.87219	0.764	0.550	15.881	11.322	6.224	-2.627	
U23	32.57	1037.518	605386.350	50.579	269.6415	25.98909	0.798	0.539	12.491	7.934	2.827	-6.060	
U24	32.57	1019.336	597276.903	50.538	258.207	25.3309	0.778	0.538	14.721	10.287	5.317	-3.332	
U25	32.57	1021.198	574548.877	51.472	243.1343	23.80873	0.731	0.548	19.550	15.223	10.384	1.977	
U26	32.57	1036.804	608878.114	50.398	265.0133	25.5606	0.785	0.537	13.995	9.545	4.557	-4.126	
U31	32.57	1020.948	573778.356	72.124	213.4838	20.91035	0.642	0.768	21.077	13.705	5.897	-7.080	-11.053
U32	32.57	1019.834	570772.061	72.257	235.6102	23.1028	0.709	0.769	12.720	4.547	-4.106	-18.48	
U33	32.57	1020.35	570762.506	72.282	221.7255	21.73034	0.667	0.770	17.890	10.198	2.055	-11.48	
U34	32.57	1021.3	573504.991	72.141	219.795	21.5211	0.661	0.768	18.762	11.171	3.132	-10.23	
U35	32.57	1022.656	575875.840	72.028	209.895	20.5245	0.630	0.767	22.585	15.367	7.720	-4.992	
U36	32.57	1023.836	576482.767	72.037	228.2595	22.29454	0.685	0.767	15.904	8.061	-0.247	-14.06	
U41	32.57	1015.86	572202.370	92.750	147.9457	14.56846	0.447	0.988	33.667	26.062	18.259	5.532	-7.985
U42	32.57	979.84	563390.676	92.510	180	18.37035	0.564	0.985	16.565	7.005	-2.805	-18.80	
U43	32.57	982.094	557622.340	92.214	175.0717	17.82637	0.547	0.982	19.298	10.057	0.575	-14.89	
U44	32.57	1011.776	570444.530	92.662	172.6215	17.06124	0.524	0.987	22.382	13.485	4.356	-10.53	
U45	32.57	1019.704	569445.832	93.036	160.2217	15.71257	0.482	0.991	28.222	19.988	11.540	-2.24	
U46	32.57	1008.464	569458.540	92.539	166.75	16.53505	0.508	0.985	24.877	16.268	7.435	-6.972	
U51	32.57	991.154	557937.228	113.267	124.1115	12.52192	0.384	1.206	26.929	19.029	10.769	-2.870	-2.115
U52	32.57	942.63	525451.941	113.788	110.2763	11.69879	0.359	1.212	31.279	23.874	16.124	3.322	
U53	32.57	989.116	558377.940	113.109	125.6955	12.70786	0.390	1.204	25.992	17.983	9.611	-4.211	
U54	32.57	973.938	550082.806	113.089	124.5075	12.78392	0.393	1.204	25.568	17.512	9.091	-4.812	
U55	32.57	986.966	561843.553	113.172	124.8045	12.64527	0.388	1.205	26.297	18.325	9.989	-3.772	
U56	32.57	946.066	531414.626	113.350	115.449	12.20306	0.375	1.207	28.714	21.012	12.956	-0.346	
U61	32.57	989.548	559962.604	123.289	104.7075	10.58135	0.325	1.313	29.862	22.785	15.273	2.746	1.669
U62	32.57	989.836	559233.497	123.384	104.5095	10.55826	0.324	1.314	29.930	22.864	15.364	2.855	
U63	32.57	1000.166	559427.710	123.910	102.2077	10.21907	0.314	1.319	31.728	24.871	17.586	5.429	
U64	32.57	984.374	552857.114	123.648	110.1525	11.19011	0.344	1.317	25.489	17.990	10.027	-3.258	
U65	32.57	971.05	545661.409	123.732	101.1683	10.41844	0.320	1.318	30.553	23.568	16.150	3.773	
U66	32.57	951.584	534118.162	123.728	104.6085	10.99309	0.338	1.318	26.725	19.356	11.528	-1.531	

4. NUMERICAL ANALYSIS

Analysis of any realistically compressed member, with realistically curved axis, made of real material that has determined structural imperfections - condition of residual stresses and variation of ultimate yield limit in individual cross section points, imply both a deformation and a stability problem. Numerical analysis within this paper is based on finite element method and PAK- software. Finite element used for description of centrally compressed member is based on a beam element of deformable cross section and general geometry. This general element can be used for linear and nonlinear (geometrical and material nonlinearity). First assumption, when describing the structure, made by this element is that it requires, one axis (longitudinal) along which the structure is constant, in geometrical and material sense (Fig. 7.a). In its plane, cross section can have arbitrary shape and material (Fig. 7.b). Nodes are assigned on reference axis of the

beam that coincides with longitudinal axis. Basic assumption is that each of these elements, that can have complex structure, can be modeled by isoparametric subelements (Fig.7c.) Since beam element comprises of subelements

(isoparametric 3D, shell and beam) it can be regarded as superelement. Cross sections of each subelement can be noticed within representative cross section (Fig.7d.). Segments are depicted by nodes that lay in the representative cross section's plane and their position is defined based on coordinate system linked to main beam nodes (Fig.8). Main beam nodes have usual beam degrees of freedom, three translations and three rotations. They are taken into account during calculation of number of equations for the structure as a whole. These are usual degrees of freedom for isoparametric elements 3D, shell and beam, and they are defined relative to the coordinate systems of the main beam nodes.

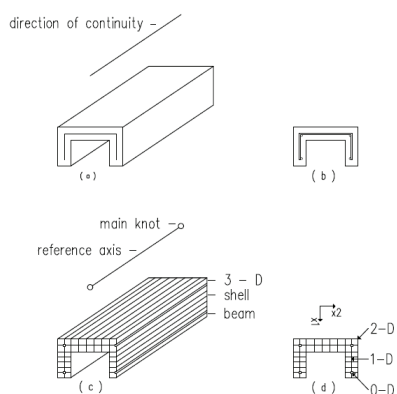


Fig. 7. Complex structure modeling with beam superelement.
 a) longitudinal axes
 b) cross section
 c) subelements of the beam superelement
 d) segments within representative cross section

SUBELEMENT		SEGMENT	
TYPE	SECTION	TYPE	FORM
3D		2D	
SHELL		1D	
BEAM		0D	

Fig. 8. Types of subelements.

5. DESCRIPTION OF THE FEM DISCRETIZATION OF THE COLUMN

One-half of the column's cross section is modeled with 26- 2D segments, as shown in the Fig. 9. Length of individual elements in these models is constant along the columns axis. The Table 1. gives the sample member lengths for numerical simulation, number of elements along the columns length and total number of elements. Fig. 9 depicts a numerical model of the member of the sample U21 and a detail with cross section and element layers along the length. Cross section is symmetrical, deformation (buckling) is assumed only in one plane so only one half of the cross section is modeled. Since deformation (buckling) is symmetric relative to the middle of the member's length, calculations are performed only for one-half of the member's length.

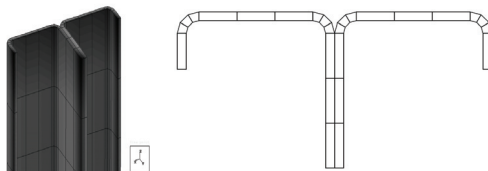


Fig. 9. Cross section (1/2 2C-profile 90.45.20.2,5) modeled with 2D segments

Beam superelement has considerable advantage, regarding fulfillment of boundary conditions, when compared to numerical models of beams and columns with shell element. Fig. 10 depicts boundary conditions that take into account symmetry conditions that prevent deflections of the column's middle plane in axial direction and lateral deflection of the column's top, as mentioned previously. Due to the nature of the force/deflection dependence, when force reaches maximum and the drops, load was simulated with predefined axial movement of the column's top. As movement control, an arc length method was used. Initial imperfections were defined according to measured values on the individual real samples that were tested up to an ultimate load state. Maximum imperfection values were varied within the numerical simulation in order to estimate its effect on the force value of ultimate load state. Initial member imperfections, in other words deviation from the straight line - longitudinal axis were defined as sine function, for simpler modeling, as follows:

$$\Delta(z) = \Delta_0 \sin(\pi z/l) \quad (1)$$

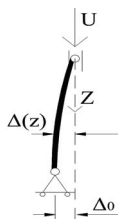


Fig. 10. Boundary conditions

Table 3. Result comparison between experimentally obtained data and numerical (FEM) simulation of the axial load capacity of complex member 2C90×45×20×2,5

Member name	Properties and number of elements		
	Length (mm)	Number of elements along the column's length	Total number of elements
U21	1,221.2	20	26*20 = 520
U33	1,709.7	28	26*28 = 728
U43	2,198.9	36	26*36 = 936
U56	2,686.7	44	26*44 = 1144
U61	2,932.0	48	26*48 = 1248

5.1. Column's material properties

Material properties for flat and corner column segments were determined experimentally in an effort to realistically take into account strengthening effects due to technological procedures of cold forming. PAK software used von Mises elastic-plastic material curve. Stress-strain curves were transformed into dependency of yield stress vs. effective plastic strain in the shape of Ramberg – Osgood curve with following expression:

$$\sigma_y(\bar{\epsilon}_p) = \sigma_y + C_y(\bar{\epsilon}_p)^n \tag{2}$$

$$n = \frac{1}{E} \quad C_y = \frac{E}{1000}$$

where σ_{y0} – is initial yield stress, C_y and n – material constants obtained from experimental data. Fig. 11 gives the σ_y/ϵ_p diagram.

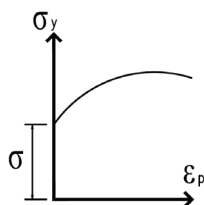


Fig. 11. Diagram σ_y/ϵ_p

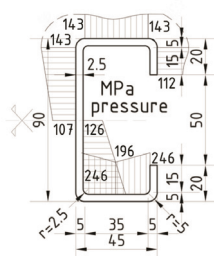


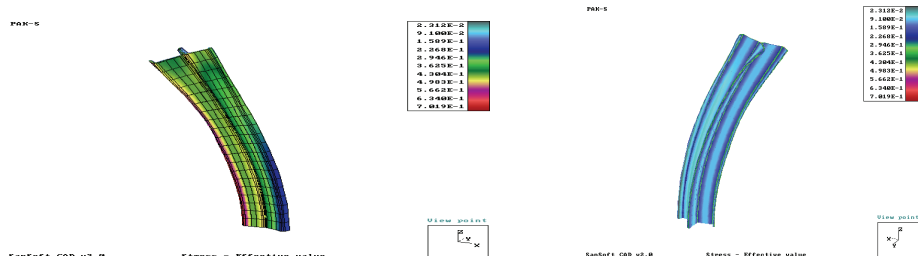
Fig. 12. Measured residual stresses

6.2. Residual stresses

Member residual stresses are defined according to experimentally obtained values and their distribution and values are given in Fig. 12. With an increase of member's axial compression plastic deformation of the material first appears in areas where residual stresses are compressive (negative), i.e. on the inner surface of the column. Influence of the residual stresses is taken into account through correction in the initial yield stresses of the compression and tension zones (Besevic, 2005).

$$\sigma_y(\epsilon_p) = (\sigma_{y0} + \sigma_{p0C}) + C_y(\epsilon_p)^n \tag{3}$$

Fig. 13 gives the numerical model shown in a state of plastic deformations over the one-half of the profile.



a) Maximal stresses - outer surface

b) Maximal stresses - inner surface

Fig. 13. Maximal stresses of the numerically modeled sample - member

Result comparison between numerical simulations and experimental testing of the centrically compressed members (Fig. 14).

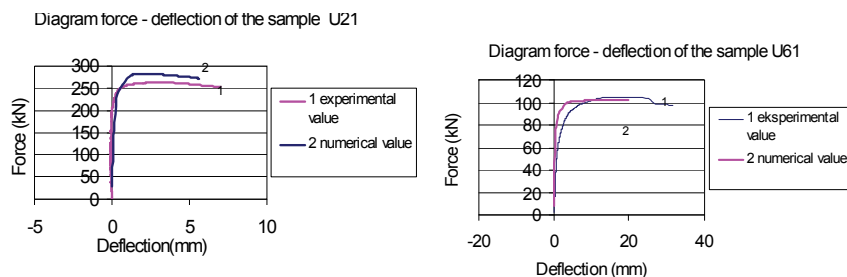


Fig. 14. Result comparison between numerical simulations and experimental testing of the centrically compressed members.

Table 4. Result comparison between experimentally obtained data and numerical (FEM) simulation of the axial load capacity of complex member 2C90×45×20×2,5

uzorak	A (mm ²)	λ_0	P_E (kN)	σ_E (kN/cm ²)	P_N (kN)	σ_N (kN/cm ²)	$\frac{\sigma_N}{\sigma_E}$ (kN/cm ²)	%	λ	κ
U21	1021.62	51.67	263.18	25.76	281.55	27.56	1.07	6.98	0.56	0.85
U33	1020.35	72.28	221.73	21.73	221.76	21.73	1.00	0.02	0.78	0.67
U43	982.09	92.21	175.07	17.83	162.44	16.54	0.93	-7.22	0.99	0.51
U56	946.07	113.35	115.45	12.20	117.48	12.42	1.02	1.76	1.22	0.38
U61	989.55	123.29	104.71	10.58	102.32	10.34	0.98	-2.28	1.33	0.32

Analysis of the numerical results yielded values of the buckling curves. Buckling curve and its numerical values are shown in Fig. 15. The same figure shows experimentally determined buckling curve and it proves that averaged values of experimental buckling curve (six series for each slenderness value) and numerical buckling curve have very high level of conformity. Numerical values of the buckling curve show that complex 2C profile must be calculated depending on its length, i.e. slenderness for same boundary conditions and same cold forming technology. For moderate slenderness values ($\lambda=70, 90$) members that were formed with this technology and with complex cross section must be calculated so that they are associated with C buckling curve. For higher slenderness values ($\lambda=110, 120$) (loss of stability appears before plastic deformations - excessive deformations) complex members must be calculated so that they are associated with a buckling curve D. For lower slenderness values, additional research must be performed in order to precisely define their buckling curve (it is suggested, for safety reasons, to make calculations associated with the buckling curve D).

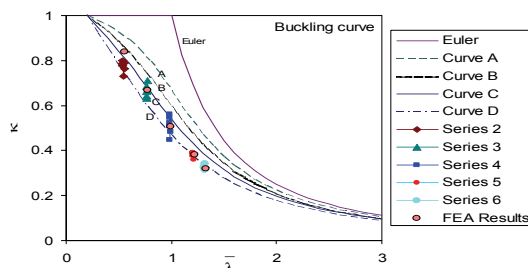


Fig. 15. Buckling curves of complex member obtained experimentally and numerically

6. CONCLUSION

Analysis within this paper included the parameters that influence the bearing capacity of centrally compressed members, what included behavior of stainless, high grade and carbon steel elements. These parameters included: increased mechanical properties - strength of cold formed profiles as a result of forming process especially in the corners, distribution, type and value of residual stresses as a result of induced strains during production. Measurements of residual stresses are in favor of rectangular distribution of stresses along the wall thickness - compression on one side, tension on the opposite side. Initial geometric imperfections were measured and analyzed within compression tests. Analysis included cold formed carbon steel columns. The columns were formed from two "C" shape profiles joint together with spot welding. Comparison of results was made against the European Codes and against the results obtained for stainless steel columns. The most significant conclusion is that this type of member has, without a doubt, be design according to the buckling curve "C" for moderate slenderness values ($\lambda=70$ and 90), for buckling curve "D" for higher slenderness values ($\lambda=110$ and 120). It is recommended to use buckling curve "D" for slenderness values $\lambda=50$, provided that the yield limit is obtained from stub column test (σ_T). If the determination of the buckling curve of the centrally compressed member with complex cross section is conducted according to the yield limit (Rel), obtained from the tensile coupon tests of the base sheet, then design has to include buckling curve "B" for slenderness values ($\lambda=70$ and 90), and for higher slenderness values ($\lambda=110$ and 120) as well as for slenderness $\lambda=50$ buckling curve "C". Analysis of above leads to following conclusions:

All experimental analyses (six series) are verified numerically. Numerical analysis was conducted with real geometric cross section properties and initial curvature of tested samples. Numerical simulation included real values of yield limit and measured distribution of residual stresses along the cross section. Appropriate buckling curves can be determined by interpolation between the five curves that were experimentally determined. Graphical representation of the obtained results is given in the Fig. 20, together with curves defined within EC. Differences of the experimental results and buckling curves A, B, C and D are clearly noted in tables and given in a form of percentage. Results obtained by the experiments and numerical simulation for the bearing capacity cold formed members with complex cross section $2C90 \times 45 \times 20 \times 2,5$ are shown in The influence of residual stresses has to be taken into account for determination of bearing capacity of compressed members since it effect its global stability. Based on these conclusions a general conclu-

sion can be made that the behavior of high grade and stainless steel centrally compressed members is similar as in carbon steel columns.

REFERENCES

1. Ultimate capacity of innovative cold-formed steel columns. S.Narayanan, M.Mahendran./Journal of constructional steel research./2003/-/489-508/-1.1-
2. Load-carrying capacity of high-strength steel box-section I-: Stub columns./Lei Gao, Hongcai Sun, Fengnian Jin, Hualin Fan/Journal of constructional steel research./2008/ doi:10.1016/j.jcsr.2008.07.002-7-
3. Test of cold high strength stainless steel compression members, Ben Young, Wing-Man Lui, Thin – Walled structures/2006,224-234/
4. Buckling analysis of high strength stainless steel stiffened und unstiffened slender hollow Section columns/Ehab Ellobody/Journal of constructional steel research./2006-/145- 155/ -5-,
5. Behavior of tubular steel members under cyclic axial loading,J.M.Goggins, B.M. Broderick, A.Y.Elghazouli, A.S.Lucas, Journal of constructional steel research.../2006-/121131/ -1-
6. The European standard family and its basis/Gerhad Sedlacek, Christian Muler/Journal of Constructional steel research./2006/1047-1059/ -4-
7. Eurocode 3: EN 1993-1-1:2005:E, Design of steel structure –part 1-1 General rules and rules for buildings /European Committee for Standardization,2004 /
8. Eurocode 3: EN 1993-1-8:2005:E, Design of steel structure –part 1-8 Design of joints /European Committee for Standardization,2004 /
9. PAK - Program for Structural nonlinear Analysis/Faculty of Mechanical engineering in Kragujevac, Serbia / M. Kojić, R. Slavković, M. Živković, N. Grujić: 1992.
10. Experiments on stainless steel hollow sections – Part 1", Material and cross-sectional behavior", Journal of Constructional Steel Research /1291-1318/. L.Gardner, D.A. Nethercot, (2004).
11. Bearing capacity of cold formed high quality stainless steel members under end axial compression, IZGRADNJA- Serbia./7-8/, (Besevic 2010).

EKSPERIMENTALNO-NUMERIČKA STUDIJA NOSIVOSTI CENTRIČNO PRITISNUTIH ŠTAPOVA OD HLADNOOBLIKOVANIH ČELIČNIH PROFILA

Miroslav Bešević, Danijel Kukaras

Analiza rezultati numeričke simulacije su granična sila, odgovarajuća pomeranja-ugibi štapa sredine uzorka i krive izvijanja štapova. Sprovedena su i obimna eksperimentalna ispitivanja nosivosti štapova pri izvijanju. Eksperimentalna ispitivanja nosivosti obuhvatila su pet serija od šest uzoraka sa vrednostima vitkosti 50, 70, 90, 110 i 120. Pritisnuti prosti štapovi analizirane su kroz Amsler testove u kojima su korišćeni sferni oslonci. Korišćena je nova elektronska oprema i originalni softveri. Pored merenja nosivosti i deformacija beleženi su i rezultati istezanja u 18 do 20 tačaka duž poprečnog preseka.

Analizirani su i rezultati najnovija istraživanja različitih autora iz ove oblasti za visokovredne i nerđajuće čelike i izvršena su poređenja.

Ključne reči: *pritisnuti štapovi, eksperimentalna analiza, numerička analiza, metod konačnih elemenata, krive izvijanja, čelik, hop-profili, nerđajući čelik, čelik visoke čvrstoće.*